Full polarization control of fiber-delivered light in a dilution refrigerator

Phoenix, Jason; Gaudreau, Louis; Korkusinski, Marek; Zawadzki, Piotr; Bogan, Alex; Studenikin, Sergei; Williams, Robin L.; Sachrajda, Andrew S.

Publisher's version / Version de l'éditeur:
https://doi.org/10.1063/5.0012174
Review of Scientific Instruments, 91, 8, pp. 1-10, 2020-08-19

Review of Scientific Instruments

Full polarization control of fiber-delivered light in a dilution refrigerator

Cite as: Rev. Sci. Instrum. **91**, 083107 (2020); https://doi.org/10.1063/5.0012174
Submitted: 28 April 2020 . Accepted: 02 August 2020 . Published Online: 19 August 2020

Jason Phoenix, Louis Gaudreau, Marek Korkusinski, Piotr Zawadzki, Alex Bogan, Sergei Studenikin, Robin L. Williams, and Andrew S. Sachrajda

Review of Scientific Instruments ARTICLE scitation.org/journal/rsi

Full polarization control of fiber-delivered light in a dilution refrigerator

Cite as: Rev. Sci. Instrum. 91, 083107 (2020); doi: 10.1063/5.0012174
Submitted: 28 April 2020 • Accepted: 2 August 2020 •
Published Online: 19 August 2020

Jason Phoenix,[a] Louis Gaudreau,[b] Marek Korkusinski, Piotr Zawadzki, Alex Bogan, Sergei Studenikin,[a] Robin L. Williams, and Andrew S. Sachrajda

AFFILIATIONS

Emerging Technology Division, National Research Council, Ottawa, Ontario K1A 0R6, Canada

[a]**Also at:** Department of Physics and Astronomy, University of Waterloo, Waterloo, Ontario N2L 3G1, Canada.
[b]**Author to whom correspondence should be addressed:** Louis.Gaudreau@nrc-cnrc.gc.ca

ABSTRACT

Birefringence in optical fibers poses a challenge to controllably delivering polarized light. Strain-induced birefringence caused by bends in the fiber, vibrations, or a large temperature gradient can significantly alter the polarization, making it particularly difficult to deliver polarization states to low-temperature environments by fiber. In this paper, we investigate the transmission of polarized light through a fiber and discuss a method we have developed for delivering arbitrarily polarized light to the base stage of a dilution refrigerator using a standard optical fiber. We have created a compact, cryogenic optical system to identify the polarization of the delivered light, while room-temperature waveplates and a mathematical fiber model are used to fully characterize and compensate for the fiber's birefringent effects. We show here that we are able to deliver horizontal, vertical, diagonal, anti-diagonal, right circular, and left circular polarization states to milli-Kelvin temperatures, with state fidelities of greater than 0.96 being achieved in all cases. Additionally, we demonstrate that we can deliver randomly selected elliptical states through a standard fiber to the refrigerator. This opens up new opportunities for fiber-based optical experiments using polarized light, such as quantum information experiments using quantum states encoded in the polarization of single photons.

https://doi.org/10.1063/5.0012174

I. INTRODUCTION

The ability of optical fibers to transmit light over long distances with minimal signal loss (~0.2 dB/km for telecom fibers) has made them a common telecommunications technology and a prime candidate for use as a means of photon delivery in quantum communication applications. It is a well-known drawback of standard optical fibers, however, that the birefringence of their cores prevents them from simultaneously preserving all polarization states. As fibers tend not to depolarize the light they transmit, it is possible to compensate for the coherent, unitary transformations they perform on the polarization so that the desired state can be accurately delivered.[1–4]

Adjustment of the output polarization can be performed using polarization controllers,[1–5] which twist, bend, squeeze, or stretch the fiber, thereby controllably altering its birefringence.[6] Electronic versions of these devices employ feedback and optimization systems to manipulate the fiber and produce the appropriate polarization at the fiber output. Compensation for a fiber's effects on polarization is often achieved by transmitting an ancillary signal with a known polarization. The second signal provides a measure of the change in fiber birefringence and acts as a reference when attempting to correct the output polarization. Some of the schemes that are used to perform these corrections include temporal multiplexing,[2,3,7] wavelength multiplexing,[1,2,4] and two-fiber systems, where the reference pulses are transmitted along a secondary channel neighboring the primary.[2,5] The overall efficiency and success of these schemes depend upon factors such as the fiber's length and external environment, and as such, they may be ill-suited for the extreme conditions of cryogenic experiments. Even polarization-maintaining (PM) fibers preserve just two states at room temperature and are not guaranteed to preserve polarization when exposed to cryogenic temperatures, as the stresses induced by cooling can be on the same order as the artificial stresses designed to maintain the polarization.[8]

Much of the literature on transmitting polarized light via optical fiber deals exclusively with linear polarization states at the fiber

output.[1–4] These systems, which often use polarizers or polarization-maintaining fibers to ensure perfectly linear output, are not concerned with the phase difference between the x and y components of the electric field.

In this paper, we will explore a system for delivering any polarization state, including elliptical and circular states, to the lowest-temperature stage of a dilution refrigerator via a standard, 30-m long, single mode optical fiber. A compact optical setup installed in the refrigerator allows us to accurately identify the polarization of light reaching the cryogenic sample space, while milli-Kelvin temperatures are maintained. The effects of the fiber on the polarization are modeled mathematically by sending known states into the fiber and comparing them to the corresponding output states. Waveplates (half-wave and quarter-wave) are used to compensate for the birefringent fiber core so that high-fidelity, arbitrary polarization states can be delivered from room temperature to the bottom of the refrigerator while operating at milli-Kelvin temperatures. This system can therefore be used as a tool by those performing optical experiments with polarized light in extreme environments.

II. SYSTEM DESCRIPTION

A. Experimental setup

To deliver polarized light through a standard optical fiber and verify delivery of the desired states, we have designed and constructed the system depicted in Fig. 1. While a fiber-coupled, 980 nm, benchtop laser source (Thorlabs, S1FC980) was used during preliminary tests of this system, the results presented here were obtained using a tunable Ti:sapphire source (Spectra-Physics, Tsunami model), with a free-space output and a wavelength tuned to about 780 nm. This wavelength was chosen because it is near the low-temperature bandgap of GaAs with which we will be working in the near future.

The laser beam is directed through a linear polarizer (Thorlabs, LPNIR050) to produce pure linear polarization. We label this polarizer P1 to distinguish it from the polarizer in the fridge. It is followed by a half-wave plate (Thorlabs, AHWP05M-980) and a quarter-wave plate (Thorlabs, AQWP05M-980), both mounted on computer-controlled mechanical rotators. The combination of these two elements, which we label HWP and QWP1, respectively, allows for the generation of any polarization state at the input of the fiber. A collimator (Thorlabs, TC06APC-780) couples the free space beam directly into a 50:50 fiber beam splitter (Oz Optics, Part No. FUSED-12-850-5/125-50/50-3A3A3A-3-1). This beam splitter is used in conjunction with a photodiode (Thorlabs, S130C) to monitor the intensity of light entering the fiber. As we will discuss in Sec. II B, the intensity measurements made by this photodiode, which we label PD1, allow us to filter out power fluctuations from the data during post-processing. Following the beam splitter is a 30-m long, 780HP, single mode fiber from Thorlabs, which transmits the light from our optics lab to the refrigerator in our cryogenics lab.

With all of the experimental components installed in the dilution refrigerator (Bluefors, BF-LD250), the system reaches a base temperature of under 10 mK. Polarized light is transmitted from the top of the refrigerator at room temperature to the mixing chamber (MC) flange by a single mode S630-HP fiber. A lensed fiber (Adamant, SLF R4 SMF FC/APC) delivers the light to our custom-built cryogenic optical setup, which is thermally coupled to the MC flange. The total length of these fridge fibers is ~2.5 m. The lensed fiber has an expected focal length of 8 μm and an estimated spot size, which is roughly 0.75 μm–1.0 μm in diameter (see the supplementary material for images of our cryogenic experimental setup).

Three piezoelectric positioners from Attocube Systems (two ANPx101/RES and an ANPz101/RES) provide sub-micron positioning of the lensed fiber in the x, y, and z directions. The positioners are used both to focus light on our samples and to direct the beam toward a compact optical setup for polarization identification. It consists of a zero-order quarter-wave plate (Thorlabs, WPQ05M-808), a linear polarizer (Thorlabs, LPNIR100), and a photodiode (Thorlabs, FDS1010). The quarter-wave plate, which we label QWP2, is mounted on a piezoelectric rotator (Attocube, ANR240/RES). The polarizer (labeled P2) is aligned with P1. The photodiode (labeled PD2) responds to light even without a reverse bias applied, so the bias is set to 0 V during our experiments in order to reduce Joule heating. PD2 maintains a linear relationship between the power of the incident light and the resulting photocurrent for power levels ranging from 0 μW to ~30 μW. By measuring the intensity of the light passing through P2 as a function of the QWP2 angle, this cryogenic optical setup allows us to accurately identify the polarization of the light exiting the lensed fiber.

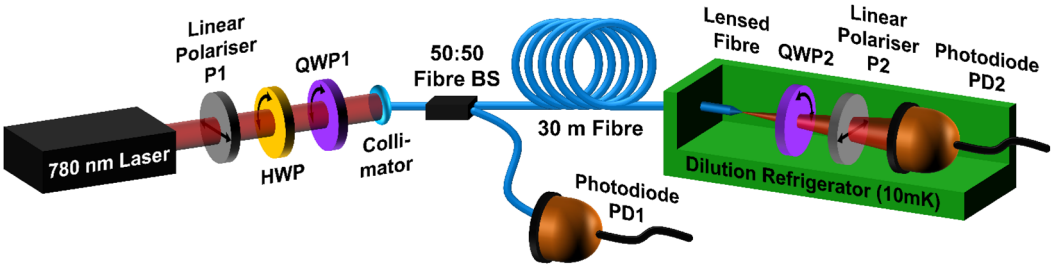

FIG. 1. A schematic of the major components used to deliver polarized light to a dilution refrigerator by fiber. A 50:50 fiber beam splitter (BS) allows us to monitor the intensity of the light entering the fiber. The final three components (QWP2, P2, and PD2) form our polarization identification system. The curved arrows on the waveplates represent the fact that they are mounted on rotators, while the horizontal arrows on the linear polarizers indicate their polarization direction (i.e., horizontal).

B. Setup details

In the first section of our room-temperature setup, a free-space laser beam travels through a polarizer, a HWP, and a QWP. We define the polarization to be in the "horizontal" state after the light has passed through polarizer P1. To simplify the mathematical simulation of the system, we attempted to manually align P1 and P2. With the two polarizers in series, a rotating HWP placed between them was used to show that there was still a residual 0.11° offset after the alignment procedures.

The retardance of a waveplate is generally dependent upon the wavelength and the angle of incidence of the laser beam. For a wavelength of 780 nm, the retardances of HWP and QWP1 were measured to be 182.5° and 90.4°, respectively, rather than the ideal values of 180° and 90°. These minor imperfections are taken into account by our simulations and do not have any noticeable effect on our ability to deliver the appropriate states through the fiber.

As mirrors induce a slight change in polarization, there are no mirrors placed between P1, HWP, and QWP1. Mirrors are used after the waveplates to help couple the free-space light into the fiber. We account for these mirrors and the collimator in our simulation by considering their polarization-altering effects to be caused by the fiber. As we shall discuss below, our model simulates the fiber as a long series of rotated retarding plates, so we can incorporate into its representation any other components, which might affect the polarization, such as the collimator or the lensed fiber.

These experiments rely heavily on our ability to use PD2 for measuring the intensity of the light passing through P2. In Fig. 2(a), for example, we see the intensity of the light measured by PD2 as a function of QWP2's rotation angle. Fluctuations in the intensity data can be caused by noise in the power output of the laser or by a wobbling of the beam path as the room-temperature waveplates rotate. This noise hinders our ability to accurately identify the polarization state and characterize the fiber's effects on polarization. To resolve this issue, a fiber beam splitter and additional photodiode (PD1) were installed in front of the 30 m fiber, as shown in Fig. 1. This setup allows for monitoring of the light intensity entering the fiber without affecting the polarization of the light reaching the sample space. For each intensity measurement we make in the fridge, an PD1 measurement is also made of the light intensity entering the fiber system. Figure 2(b) shows the PD1 data that were recorded at the same time as the data in panel 2(a). To eliminate the noise from the PD2 measurements, we calculate the ratio of each PD1 data point to the average PD1 intensity and then divide the corresponding PD2 datum by that ratio. We may summarize this with the following equation:

$$\mathrm{PD2}_i^{\mathrm{corrected}} = \mathrm{PD2}_i^{\mathrm{measured}} \frac{\sum_{j=1}^{n} \mathrm{PD1}_j / n}{\mathrm{PD1}_i}, \tag{1}$$

where PDX_i is the intensity measured by photodiode X for a given QWP2 angle i and n is the total number of data points. The result is a re-scaling of the polarization data with respect to the average and a correction of all noise originating from the room-temperature setup in front of the fiber. Figure 2(c) shows the same data as in Fig. 2(a) after Eq. (1) has been used to remove the noise. We note that before post-processing, the average signal-to-noise ratio in our data can be as low as 6, while it is about 75 afterward. Hence, we conclude that most of the noise in the system appears to originate from the room-temperature components in front of the fiber. The fiber itself and the refrigerator setup appear to introduce very little noise into the polarization, even though the pulse-tube refrigerator generates some small vibrations.[9] The cryogen-free dilution refrigerator used in these experiments maintains a stable temperature gradient along the fiber, which resolves the potential issue of temperature fluctuations experienced by wet dilution refrigerators due to changing helium bath levels.

The fiber used in our setup is a standard, single mode fiber with no built-in polarization-maintaining stressors. PM fibers only

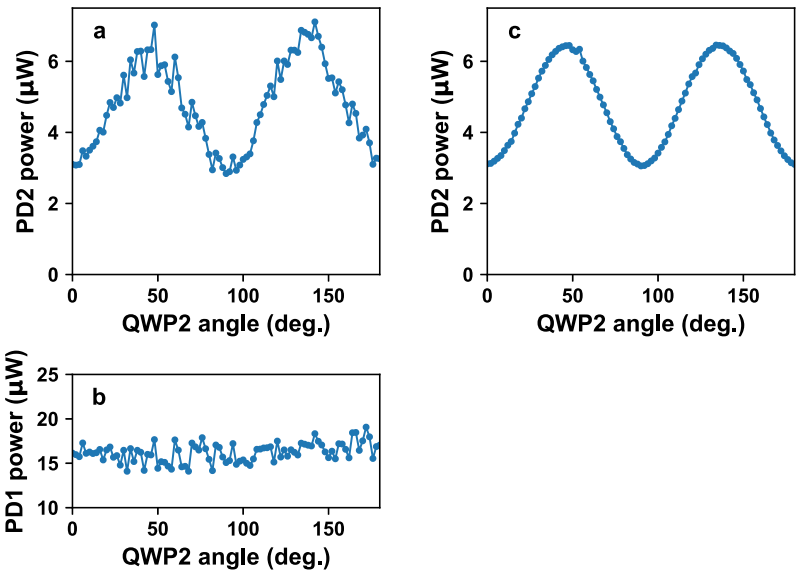

FIG. 2. (a) Measured PD2 data showing noise due to laser intensity fluctuations. (b) Intensity of light entering the fiber system, as measured by PD1. Note how the noise matches the noise in panel (a). (c) The same dataset as in panel (a) after post-processing. Equation (1) and the data in panel (b) were used to eliminate intensity noise.

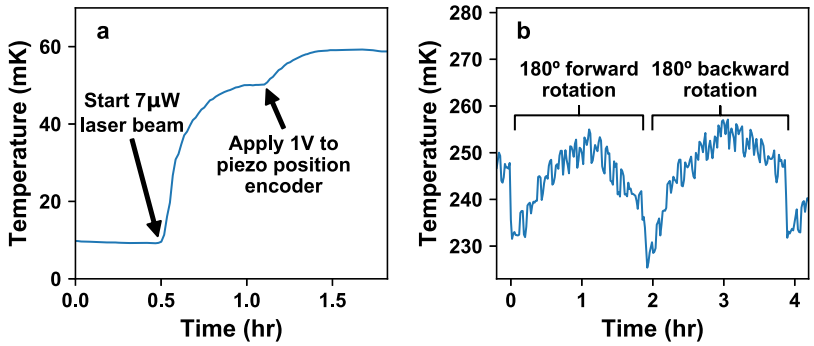

FIG. 3. Fridge heating during polarization tests. (a) Temperature increasing from base temperature (10 mK) first due to presence of laser beam and, then, the application of 1 V to the piezoposition encoder. (b) Heat dissipation in MC due to rotation of QWP2.

preserve the two perpendicular linear polarizations that are aligned with the core's fast and slow axes, i.e., the horizontal and vertical states. All other polarizations, however, will be projected onto these two modes, each of which travels at a different speed. The result is that one cannot use PM fibers to send diagonal, circular, or elliptical polarizations[10,11] (specially designed "spun" optical fibers with rotating, bow-tie-shaped stressors preserve circular polarization, but there are no fibers that will preserve all polarization states simultaneously).

Temperature fluctuations can have major short-term effects on the polarization at the fiber exit,[5] so proper thermal anchoring of the fiber is key to preventing a wandering output state. This is achieved in our system by anchoring the fiber between gold plates at each stage in the fridge. The majority of the remaining experimental apparatus in the refrigerator consists of a single unit (bolted together) containing all mechanical, electrical, and optical components. Great care was taken in the thermal anchoring of these components in order to sustain milli-Kelvin temperatures during experiments. The experimental components are mounted on a custom-made brass plate (1/16 in. thick, 4.64 in. maximum width), which has a specially designed pattern of holes and slots to minimize Joule heating due to eddy currents in the presence of a changing magnetic field. The brass plate is connected to a 1/4in. thick copper ring by three thin-walled, stainless steel tubes (1/2 in. diameter, 12.4 in. long), which are positioned at 120° intervals around the ring for mechanical stability. The copper ring is bolted to the bottom of the MC flange in the refrigerator, and the stainless-steel tubes center the experimental apparatus within an 8 T, 5 in. bore, superconducting magnet. As the thermal conductivity of the stainless-steel tubes is too low at millikelvin temperatures, the brass plate and all experimental components are thermally linked to the copper ring (therefore to the MC) by an oxygen-free copper cable (4 mm diameter), screwed down at both ends. All wiring from the components and sample is also thermally connected to the MC via a copper thermal sink bolted to the copper ring.

This extensive thermal anchoring is necessary to reduce the heating effects of the polarization experiments themselves. The intensity of light exiting the lensed fiber in the refrigerator was ~6.5 μW–7 μW during our experiments, as measured by PD2 at low temperatures. When operating the refrigerator at low temperatures, this laser power has the effect of increasing the MC temperature from base temperature up to 50 mK. Additionally, the MC temperature increased from 50 mK to 60 mK when 1 V was applied to the resistive encoder of QWP2's piezoelectric rotator, which was necessary for readout of the rotator's position. The temperature changes corresponding to these heat inputs are shown in Fig. 3(a). Further heating is caused by the rotator's movement during experiments, requiring us to navigate the trade-off between heat dissipation and rotator speed. Figure 3(b) demonstrates the heating caused by two consecutive polarization identification tests, which raised the temperature to ~250 mK due to heat dissipation by the rotator.

III. MODELLING AN OPTICAL FIBER'S EFFECTS ON POLARIZATION

Complete characterization of the fiber's birefringent core is required in order to calculate in advance the waveplate orientations that produce the desired polarization state at the fiber output. We begin by considering the mathematical model of a general retarding material. The standard representation of a retarding material, such as a waveplate, takes the following form when written using Jones matrices:

$$\begin{aligned} M &= R(-\theta)D(\phi)R(\theta) \\ &= \begin{bmatrix} \cos\theta & -\sin\theta \\ \sin\theta & \cos\theta \end{bmatrix} \begin{bmatrix} e^{-i\phi/2} & 0 \\ 0 & e^{i\phi/2} \end{bmatrix} \begin{bmatrix} \cos\theta & \sin\theta \\ -\sin\theta & \cos\theta \end{bmatrix}, \end{aligned} \tag{2}$$

$D(\phi)$ is a waveplate matrix with a phase delay of ϕ (in radians) and a fast axis oriented horizontally. $R(\theta)$ is a standard 2×2 rotation matrix that translates between the reference frames of the lab and waveplate. M therefore represents a retarder with a fast axis, which has been rotated by an angle θ from the horizontal.

The fiber's effects on polarization can be described mathematically by considering the fiber to be composed of a long series of n retarding plates.[10] Each plate M_i has a unique retardance ϕ_i and a fast axis rotated by an angle θ_i from the horizontal. The fiber matrix F may then be written as

$$\begin{aligned} F &= M_{n-1}M_{n-2}\ldots M_2M_1M_0 \\ &= R(-\theta_{n-1})D(\phi_{n-1})R(\theta_{n-1})R(-\theta_{n-2})D(\phi_{n-2})R(\theta_{n-2})\ldots \\ &= \prod_{i=1}^{n} R(-\theta_{n-i})D(\phi_{n-i})R(\theta_{n-i}). \end{aligned} \tag{3}$$

When written using Mueller matrices, it can be shown that the application of the pull-through lemma to this equation reduces it to the following simplified result,[10]

$$F = R(-\theta_a)D(\phi)R(\theta_b). \tag{4}$$

Solving for the three fiber parameters θ_a, θ_b, and ϕ is achieved by sending known polarization states into the fiber and comparing them to the corresponding output states. Note that although Eq. (4) is reminiscent of the usual equation for a rotated retarder, as in Eq. (2), the angles θ_a and θ_b are separate variables here because we are concatenating many retarding plates. If the fiber does not cause depolarization, Eq. (4) can be written using Jones matrices instead of Mueller matrices, as was done in our experiments.

IV. DELIVERY OF POLARIZED LIGHT

Our standard procedure for delivering polarized light by fiber is comprised of the following four steps:

A. **Measure Fiber Effects:** Send known polarization states into the fiber and measure the output states.
B. **Fit Fiber Parameters:** Fit the data to the fiber model using a genetic algorithm and extract the three parameters describing the fiber (θ_a, θ_b, and ϕ).
C. **Calculate Waveplate Orientations:** Calculate the HWP and QWP1 orientations required to compensate for the fiber effects.
D. **Verify Delivery of States:** Verify that the fiber has been accurately characterized by delivering specific polarization states to the refrigerator and identifying them.

In Secs IV A–IV C, we will elaborate upon each of these four steps to provide a detailed description of our process.

A. Measure fiber effects

To determine how the fiber affects polarization, we begin by sending known states into the fiber and measuring the resulting output states. The input states are prepared using the HWP and QWP1 in front of the fiber, while the output states are identified in the fridge by using PD2 to measure the amount of light that passes through the cryogenic polarizer P2 as a function of QWP2's rotation angle. This combination in the fridge of a rotating quarter-wave plate, a linear polarizer, and a photodiode is sufficient to uniquely identify every polarization state (see the supplementary material for a proof of this claim).

Characterizing the fiber's behavior is therefore achieved by creating a "polarization map" of the measured intensity at PD2 as a function of the QWP1 and QWP2 angles. This is done for several orientations of the HWP. Figures 4(a) and 4(b) depict two polarization maps, each produced at a different HWP angle. Accurate characterization of the fiber's effects on polarization depends on the quality of these initial maps, so higher resolutions and additional datasets result in better fiber characterization.

There is a trade-off, however, between accurate fiber characterization and the time required to acquire these maps. In our system, the speed at which we could produce each dataset was limited by the speed of QWP2's piezoelectric rotator, which dissipates heat in the refrigerator as it rotates. At room temperature, we are able to produce a 4000-data-point map in 3 h. For identical resolution at low temperatures, each dataset requires ~7 h, and the MC temperature rises to ~140 mK during those runs.

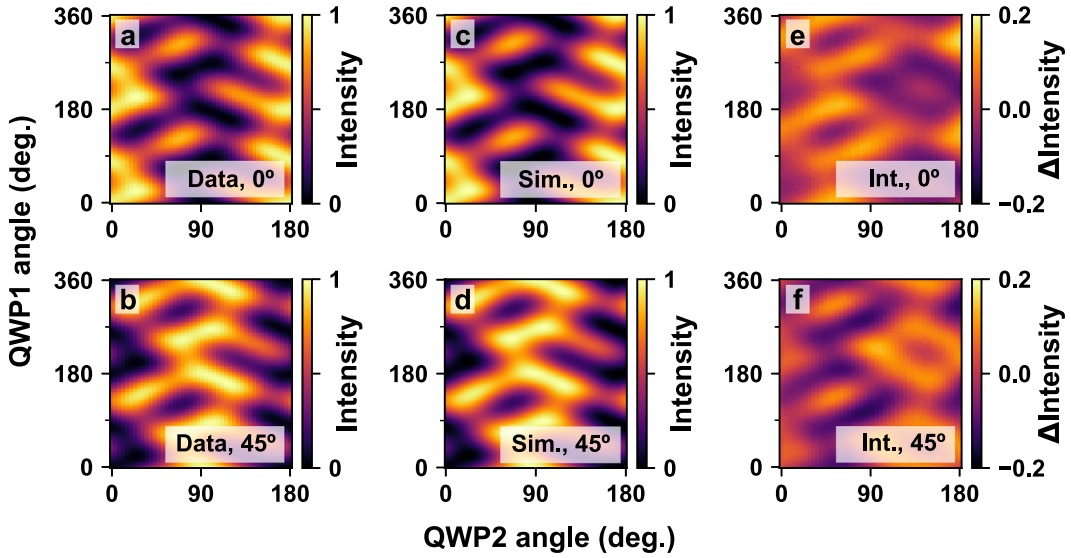

FIG. 4. Measured polarization maps produced for HWP angles of (a) 0° and (b) 45°. The corresponding simulations of these maps are shown in (c) and (d), respectively. These simulations were made after extracting the fiber parameters from the data using a genetic algorithm. Panels (e) and (f) show the intensity differences, Δ intensity, between the data and simulations for the 0° and 45° cases, respectively.

B. Fit fiber parameters

To obtain the fiber parameters, the polarization maps are fit to a model of the system using a custom-made genetic algorithm program. The algorithm simulates the optical system using Jones calculus and the fiber model discussed in the Methods section (see the supplementary material for further details on the system model). Starting with several randomly selected seed values for the unknown parameters, the program employs mutations and recombinations over many generations to evolve each set of parameters and find the values that allow the closest fit of the simulation to the data. For greatest accuracy of the results, multiple polarization maps (each produced with a different HWP angle) are loaded into the algorithm program simultaneously. Depending on the amount of data being fit, the program usually requires only 200–300 genetic iterations to solve for the fiber parameters with sufficient accuracy.

The genetic algorithm program has ten input parameters that can either be set to known values or be calculated from the data. The first seven are the three fiber parameters, the retardances of the three waveplates, and the offset angle between the two linear polarizers. The program also has three parameters that account for the offset angles between the fast axes of the three waveplates and the "0°" settings of their respective rotators. The three fiber values are typically the only variables that are fit, except in cases where we have reason to suspect that one of the other parameters has changed since it was previously measured (due to a temperature change, for example). The algorithm's remaining input parameters are measured directly and set as fixed parameters for the fitting procedure.

Once the fitted fiber values have been returned by the algorithm, we can do a preliminary test of their accuracy by using them to simulate the measured polarization maps. Figure 4 shows a comparison of low-temperature data and the corresponding simulations after fitting. The fitted fiber values for those datasets were $\theta_a = 96.96^\circ$, $\theta_b = 101.5^\circ$, and $\phi = 106.9^\circ$. The retardance of QWP2 was also fit in this case, just to verify that it was not significantly affected by the cryogenic temperatures. The fitting algorithm returned a retardance of 95.4°, which is close enough to the ideal value of 90° that we are still able to use the waveplate for accurate identification of polarization states in the refrigerator. To highlight the remarkable agreement between the data and simulation, the last two panels of Fig. 4 show the intensity difference, from which we extracted an rms difference of only 0.062 for panel (e) and 0.065 for (f).

The reliability of the polarization maps and fitted fiber parameters depends on the fiber birefringence remaining constant. Consequently, all polarization measurements are made only when the refrigerator has reached a stable temperature, and new polarization maps must be acquired and fit if there is any significant change in the state of the fiber.

C. Calculate waveplate orientations and verify delivery of states

A unique combination of HWP and QWP1 angles is required in order to deliver a specific polarization state to the fridge. Note that we are not using these waveplates to produce the inverse of the unitary transformation the fiber performs on the polarization. Instead, the waveplates are used to alter the horizontal input state (produced by P1) such that the light will have the desired polarization after passing through the fiber. The fitted fiber parameters are used to calculate the required HWP and QWP1 angles, and once the waveplates have been properly oriented, the polarized light is sent through the fiber to the dilution refrigerator.

As shown in Fig. 1, our homemade state readout system in the dilution fridge is comprised of a rotating QWP, a horizontally oriented linear polarizer, and a photodiode. Measuring the light intensity with PD2 as a function of QWP2's angle produces a unique signature for every possible polarization, allowing for accurate identification of the states exiting the lensed fiber. Figures 5(a)–5(c) show simulations of six such signatures. These six "standard" polarizations (horizontal, vertical, diagonal, anti-diagonal, right circular, and left circular) form the bases in which most polarization experiments are conducted.

As this is a novel setup, we will discuss these simulated results in more detail here (see the supplementary material for more information on how this system works). For the horizontal state, Fig. 5(a) shows that all of the light passes through the polarizer when QWP2 is at 0° (i.e., when its fast axis is aligned with polarizer P2). With the waveplate rotated by 45° from horizontal, the light reaching the polarizer has right circular polarization, so only half of it is transmitted. Passing through various elliptical states as QWP2 continues to rotate, we again get horizontal polarization at 90°, followed by left circular at 135°. The pattern repeats every 180°. Vertical polarization shows a similar pattern, although it oscillates between normalized intensities of 0 and 0.5 as the QWP transforms it from vertical to circular and back again. The diagonal and anti-diagonal states in Fig. 5(b) oscillate about a normalized intensity of 0.5 as they transition between $\pm 45^\circ$ linear and circular states, which are only half-transmitted through the horizontal polarizer. The maxima and minima in this plot are elliptical states. Finally, Fig. 5(c) shows the readout signatures for the right and left circular states, which are sinusoids with 180° periods. These signatures oscillate between normalized intensities of 0 and 1 as the rotating quarter-wave plate causes the state to shift between vertical and horizontal, passing through circular as it does so.

The measured signatures of the six standard polarizations at low temperatures (~240 mK) are displayed in Figs. 5(d)–5(f). The data are overlaid on simulated signatures (black lines), which were produced using the fitted QWP2 retardance. By comparison, the simulations shown in Figs. 5(a)–5(c) use the ideal retardances and therefore exhibit slightly different behavior. To reduce heat dissipation in the refrigerator, data were only taken for a 180° rotation of QWP2. We used the fiber splitter and PD1 to eliminate noise, and all six datasets were normalized to the maximum value of the horizontal dataset (we are able to use the horizontal state to normalize the other five because there is minimal depolarization and the lensed fiber's out-coupling efficiency is independent of the polarization).

For each of these polarizations, we were able to successfully deliver the desired state to the refrigerator at low temperatures using the unique set of waveplate angles calculated for it. Deviations of the data from the simulations in these plots are mostly attributed to slight depolarization (note how the vertical and circular states do not quite touch the "zero intensity" level) and issues with the step size/position of the QWP2 rotator. The piezoelectric rotator uses

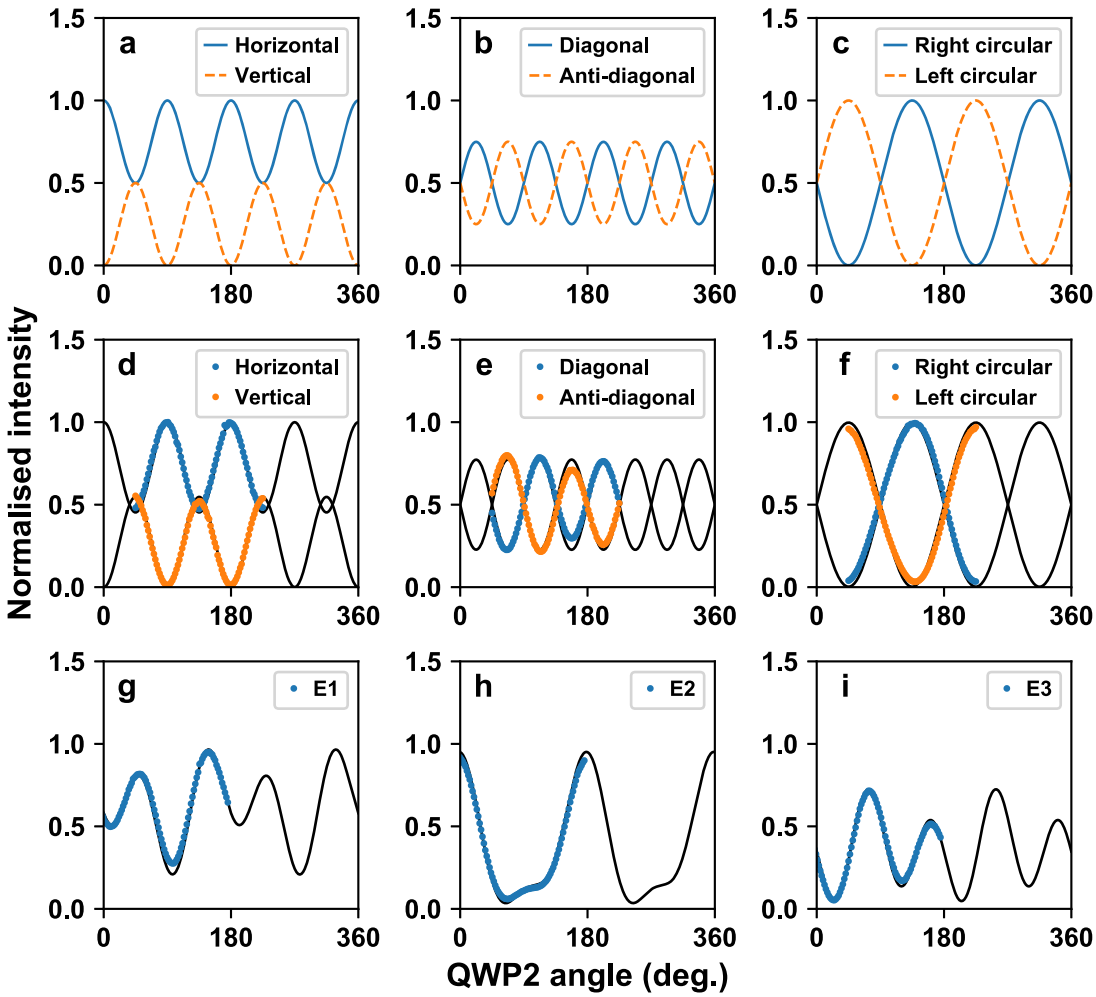

FIG. 5. Plots of the normalized intensity measured by PD2 vs QWP2's rotation angle. The top row of graphs shows simulations (using ideal waveplate retardances) of the signatures for (a) horizontal and vertical, (b) diagonal and anti-diagonal, and (c) right and left circular polarizations. The second row shows the measured low-temperature signatures for (d) horizontal and vertical, (e) diagonal and anti-diagonal, and (f) right and left circular polarizations, which are overlaid on the simulated signatures (black solid lines). The bottom row contains plots of the measured low-temperature signatures for three randomly selected elliptical states from Eq. (8): (g) E1, (h) E2, and (i) E3. The simulated signatures in the bottom two rows are produced using the fitted QWP2 retardance.

an imperfect, home-made calibration file, which can lead to minor distortion of the data.

To quantify the quality of the output states, we calculate their fidelities. For pure quantum states, the fidelity of a measured state $|\psi\rangle$ with respect to the expected state $|\phi\rangle$ is defined as

$$\mathscr{F} = |\langle\phi|\psi\rangle|^2. \tag{5}$$

Note that although we are dealing with a beam of light, which is generally described in classical terms, the lack of interaction between the individual photons in the beam allows us to apply this quantum definition of fidelity to their collective polarization. To account for depolarization, we apply a generalized definition of fidelity. The fidelity of a state with density matrix ρ with respect to an ideal state σ is defined as

$$\mathscr{F} = \left(\mathrm{Tr}\sqrt{\sqrt{\sigma}\rho\sqrt{\sigma}}\right)^2. \tag{6}$$

The equation for the fidelity of an arbitrary polarization state is excessively long when written out in full, but the fidelity equations for the six standard polarization states can be easily derived. These are summarized in Table I and are written in terms of the Stokes parameters S_1, S_2, and S_3. These represent the proportion of light that is polarized along the horizontal/vertical, diagonal/anti-diagonal, and right/left circular axes of the Poincaré sphere, respectively. As shown in in Table I, a low-temperature fidelity of greater than 0.96 was achieved for all six polarizations at low temperatures, with the horizontal state reaching a fidelity as high as 0.994. Due

TABLE I. Equations for the fidelities of the six standard polarization states, as well as the measured fidelities, for polarized light transmitted through a fiber at both room temperature and low temperature.

State	Fidelity equation	Room-temp. fidelity	Low-temp. fidelity
Horizontal	$\frac{1+S_1}{2}$	0.993 ± 0.001	0.994 ± 0.004
Vertical	$\frac{1-S_1}{2}$	0.978 ± 0.004	0.978 ± 0.003
Diagonal	$\frac{1+S_2}{2}$	0.986 ± 0.005	0.961 ± 0.007
Anti-diagonal	$\frac{1-S_2}{2}$	0.996 ± 0.005	0.964 ± 0.006
Right	$\frac{1+S_3}{2}$	0.924 ± 0.003	0.983 ± 0.002
Left	$\frac{1-S_3}{2}$	0.922 ± 0.003	0.968 ± 0.002

to the slow rotation rate of QWP2's rotator, each of the results in the table is from just a single measurement, rather than the average of multiple measurements. We should point out that the equations of Table I show that for a completely unpolarized state, in which $S_1 = S_2 = S_3 = 0$, the fidelity with respect to a fully polarized state is always 0.5.

In addition to these six common polarization states, three elliptical states were also chosen at random to verify that we could deliver arbitrary polarizations to the refrigerator. These states were defined using Stokes vectors,

$$S = \begin{bmatrix} S_0 \\ S_1 \\ S_2 \\ S_3 \end{bmatrix}, \tag{7}$$

where S_0 is the total (often normalized) light intensity. Written as Stokes vectors, our randomly chosen elliptical states are

$$\mathrm{E1} = \begin{bmatrix} 1 \\ 0.53 \\ 0.78 \\ 0.34 \end{bmatrix}, \ \mathrm{E2} = \begin{bmatrix} 1 \\ -0.49 \\ -0.2 \\ 0.85 \end{bmatrix}, \ \mathrm{E3} = \begin{bmatrix} 1 \\ -0.6 \\ 0.77 \\ -0.21 \end{bmatrix}. \tag{8}$$

Figures 5(g)–5(i) show the measured and simulated signatures for these states at the fiber exit, with the measured results closely matching the model. The successful delivery of these *randomly selected* elliptical states, in addition to the six standard states, appears to prove that our system is able to deliver by fiber any arbitrary polarization to the refrigerator at low temperatures. (Several other random elliptical states were also successfully delivered in room-temperature tests). To our knowledge, this is the first reported instance of arbitrary polarization being delivered in a controlled and predictable manner to a dilution refrigerator by an optical fiber.

The low-temperature tests in Figs. 5(d)–5(i) were conducted at 240 mK due to heating caused by QWP2's piezoelectric rotator. Now that we have confirmed the system works, future tests may be conducted using slower QWP2 rotation to reduce heating and avoid any resulting changes in fiber birefringence. Once polarization identification is complete, the refrigerator can be returned to base temperature by turning off QWP2's rotator and reducing the laser intensity. Note that the initial polarization maps and fiber characterization from Fig. 4 were done at a temperature of ~140 mK, yet we were still able to accurately deliver the desired states at a temperature of 240 mK. Additionally, the temperature cooled briefly down to 60 mK on three separate occasions, while QWP2 was stationary. This would seem to indicate that a temperature change of around 100 mK–180 mK has a minimal impact on the state of the fiber.

Finally, while this system is designed to correct the unitary transformation of the polarization by the fiber, it does not prevent depolarization. Importantly, our experiments have shown that our setup, which incorporates a 30-m long fiber, suffers from very little depolarization, so we are able to use waveplates to compensate for the unitary transformation the fiber performs on the state. It is possible, however, that longer fibers (e.g., tens of km in length) may experience a greater degree of depolarization. Using Mueller calculus for modeling the system and fitting the data should at least allow one to identify and account for depolarization, although it cannot be corrected using the system described here.

V. STABILITY OF FIBER SYSTEM

As a measure of the system's stability, the fidelity of the horizontal state was monitored over a period of ~35 h at low temperatures, as shown in Fig. 6(a). The monitoring process involved repeated acquisition of the polarization signature, followed by fitting each signature to determine the output state from the fiber. Any change in the fiber's birefringence would be observable as a change in the polarization and hence a change in the fidelity. Note that the y-axis is plotted between 0.5 and 1 to show the measured fidelity with respect to that of completely unpolarized and completely polarized states, respectively.

During our observation period, the fidelity of the horizontal state remained above 0.955 and was very stable. Accidental changes in the MC temperature that occurred during the monitoring period [Fig. 6(b)] caused a shift in the polarization from very near horizontal to the slightly elliptical state,

$$\mathrm{E} = \begin{bmatrix} 1 \\ 0.97 \\ 0.05 \\ 0.2 \end{bmatrix}. \tag{9}$$

The results of this monitoring experiment indicate that when the temperature of the cryogenic components is stable, our novel system is able to deliver a stable polarization state through a fiber at low temperatures. Interestingly, we have found that quite significant and long-lived temperature fluctuations can result in only minor changes in the output state, and the state quickly stabilizes when the temperature is fixed. Strong evidence of this was observed when the temperature changed twice during the monitoring period. First, the temperature dropped from 240 mK to 60 mK for over an hour due to the monitoring program aborting unexpectedly [see the 10-h mark

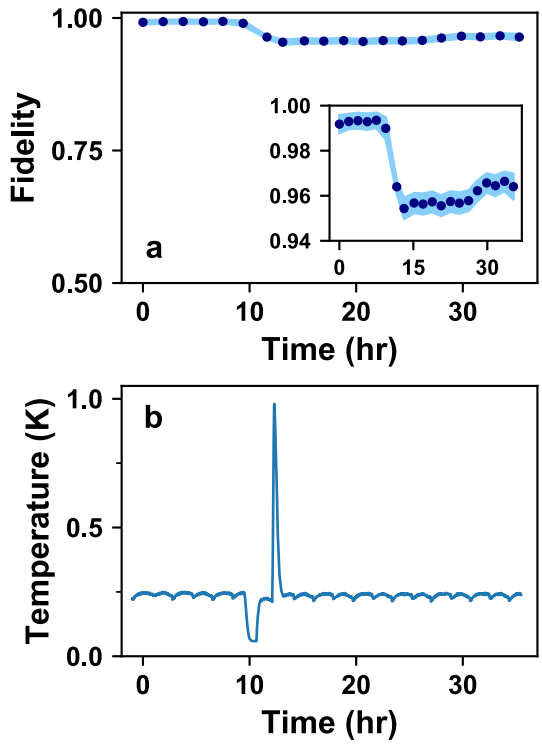

FIG. 6. (a) Fidelity of the horizontal state monitored over 35 h (dark blue points). The uncertainty of the fidelity (light blue shading) is the standard deviation in the fit of the fiber output state with respect to perfect horizontal polarization. Inset: zoomed-in view showing the small drift in fidelity over time. (b) MC temperature during monitoring period, including an unintended temperature drop to 60 mK at 10 h, shortly followed by a brief temperature increase to 1 K.

in Figs. 6(a) and 6(b)]. After re-initialization of the program, QWP2 performed one state measurement before quickly rotating 180° back to its starting position. The resulting heat output caused the temperature to increase to 1 K. This brief, yet dramatic temperature event did not significantly affect the new elliptical state, however, and after the temperature stopped changing, the new polarization state remained stable for the next 22 h. These results suggest a hysteresis effect, as the fidelity did not return to its initial value of ~0.993 after the temperature returned to 240 mK at 14 h. Therefore, the fiber did not settle back into its original state. Additionally, the decrease in temperature by 180 mK had a greater effect on the polarization than the subsequent increase by almost 1 K. The reasons for this are not known and should be explored further. We note again that these temperature fluctuations resulted in minor fidelity changes.

It should be noted that the waveplate angles used to produce the horizontal state were calculated using polarization maps obtained 2.5 days before the monitoring began. Our system was therefore stable over a total period of at least 4 days, with no indication of changes at the conclusion of the monitoring period. This high degree of stability is likely due to the relatively short length of fiber in our setup (30 m) and the controlled environment of our laboratories. Multi-kilometer-long fibers that are exposed to environmental influences such as vibrations and temperature fluctuations experience far greater polarization instability and may require more frequent fiber characterization procedures.[3,5,7] The stability of our system, however, allows us to conduct low-temperature experiments with polarized light over a period of at least several days without the need to recharacterize the fiber.

VI. CONCLUSION

In summary, we have achieved successful fiber-based delivery of polarization states to a dilution refrigerator at low temperatures, and all six standard states were delivered to the refrigerator with fidelities of >0.96. Our ability to transmit several randomly selected elliptical states, in addition to the standard six, indicates that our setup allows for delivery of any polarization state to the refrigerator. To achieve this, we have created a compact polarization readout scheme suitable for installation in cryostats and demonstrated that our system is very stable over a period of at least 4 days.

Since photons propagating in parallel tend not to interact with each other, the system presented here should function identically when single photons are used instead of a laser beam. The single photon will experience the same effects as each photon in the beam and should therefore have the same state at the fiber output. There should also be no issues associated with the difference in the travel times of the photon's electric field components propagating along the fiber's fast and slow modes because the average group delay is typically on the order of a picosecond or under for a standard, 100-km long telecom fiber.[2] Since current photodetector technology has a temporal resolution on the order of a few hundred picoseconds[1] and exciton lifetimes in semiconductor structures tend to be on the order of a nanosecond, time-bin entanglement is unlikely to arise through the use of a fiber for the transmission of individual polarized photons. Our future experiments will therefore involve the transmission of single polarized photons through a fiber at cryogenic temperatures, with initial characterization of the fiber achieved using a laser beam as described above.

SUPPLEMENTARY MATERIAL

See the supplementary material for mathematical model of the optical system and proof that the readout components in the fridge uniquely identify polarization states.

ACKNOWLEDGMENTS

J.P. and S.S. thank the Natural Sciences and Engineering Research Council of Canada for financial support. The authors would also like to thank Jeongwan Jin for helpful discussions.

The authors declare that they are preparing an application to patent the system described in this paper.

DATA AVAILABILITY

The data that support the findings of this study are available from the corresponding author upon reasonable request.

REFERENCES

[1]G. B. Xavier, G. V. de Faria, G. P. Temporão, and J. P. von der Weid, Opt. Express **16**, 1867 (2008).
[2]G. B. Xavier, N. Walenta, G. V. de Faria, G. P. Temporão, N. Gisin, H. Zbinden, and J. P. von der Weid, New J. Phys. **11**, 045015 (2009).
[3]J. Chen, G. Wu, Y. Li, E. Wu, and H. Zeng, Opt. Express **15**, 17928 (2007).
[4]A. N. Pinto, A. J. Almeida, N. A. Silva, N. J. Muga, and L. M. Martins, Proc. SPIE **8001**, 80011M (2011).
[5]J. F. Dynes, I. Choi, A. W. Sharpe, A. R. Dixon, Z. L. Yuan, M. Fujiwara, M. Sasaki, and A. J. Shields, Opt. Express **20**, 16339 (2012).
[6]OZ Optics: DTS0011 Electrically Driven Polarisation Controller-Scrambler, Ottawa, 2016, EPC data sheet.
[7]Y.-Y. Ding, H. Chen, S. Wang, D.-Y. He, Z.-Q. Yin, W. Chen, Z. Zhou, G.-C. Guo, and Z.-F. Han, Opt. Express **25**, 27923 (2017).
[8]M. J. Nelson, C. J. Collins, and C. C. Speake, Rev. Sci. Instrum. **87**, 033111 (2016).
[9]R. Kalra, A. Laucht, J. P. Dehollain, D. Bar, S. Freer, S. Simmons, J. T. Muhonen, and A. Morello, Rev. Sci. Instrum. **87**, 073905 (2016).
[10]S. Manhas, J. Vizet, S. Deby, J.-C. Vanel, P. Boito, M. Verdier, A. De Martino, and D. Pagnoux, Opt. Express **23**, 3047 (2015).
[11]N. Gisin, J.-P. von der Weid, and J.-P. Pellaux, J. Lightwave Technol. **9**, 821 (1991).